BMC Musculoskeletal Disorders

RESEARCH

Open Access

Evaluating the antimicrobial and anti-inflammatory mechanisms of dexmedetomidine in managing bone infection: a laboratory perspective

Merve Hayriye Kocaoğlu[1], Günseli Çubukçuoğlu Deniz[2], Duru Aras-Tosun[3*], Evrim Güneş Altuntaş[4] and Erkan Tuncay[5,6]

Abstract

Background Osteomyelitis involves bone destruction, impaired bone formation, and systemic inflammation. Dexmedetomidine (DXMT) possesses antioxidant, anti-inflammatory, and anti-apoptotic properties alongside sedative and analgesic effects. This study evaluates DXMT's effects on markers of infection and bone healing using osteocyte-like cells infected by *Staphylococcus aureus* (*S. aureus*).

Methods Human osteosarcoma-derived SAOS-2 cells were differentiated to an osteocyte-like phenotype over 28 days using potassium dihydrogen phosphate. Differentiation was verified via qPCR for osteogenic markers. Cytotoxicity of DXMT (0.1–10 µM) was tested using WST-1 assay and Reactive Oxygen Species (ROS) production analysis. Cells infected with *S. aureus* were treated with DXMT to assess its antimicrobial, anti-inflammatory (via ELISA for cytokines IL1-ß, TNF-α, IL-17, and IL-6), and osteogenesis-promoting effects.

Results DXMT ≤ 1 µM did not affect cell viability, while 2, 5, and 10 µM DXMT administration reduced cell counts. A 5 µM dose slightly reduced intracellular bacterial load (6.2 log in controls vs. 6.1 log with DXMT), while neither less nor more DXMT was effective on reducing the *S. aureus* load. Doses ≥ 5 µM effectively reduced ROS production and inflammation post-infection in a time-dependent manner. *S. aureus* infection decreased osteogenic markers, but DXMT mitigated cellular stress and inflammation with a positive impact on osteogenesis at therapeutic doses.

Conclusion DXMT at 5 µM is an optimal dose to reduce infection-induced cellular stress and promote bone healing in osteomyelitis in vitro, balancing antimicrobial effects and cytotoxicity.

Keywords Anti-inflammation, Antimicrobial, Dexmedetomidine, Osteoblast, Osteomyelitis, Reactive Oxygen Species (ROS), *Staphylococcus aureus (S. aureus)*

*Correspondence:
Duru Aras-Tosun
duruaras@gmail.com
Full list of author information is available at the end of the article

Introduction

Osteomyelitis, which may manifest acutely or chronically, is a bone infection that results in progressive destruction of bone tissue, decreased new bone formation, and deterioration of bone quality, accompanied by an elevated systemic inflammatory response [1, 2]. It may manifest due to direct exposure of bone tissue to the pathogen following acute trauma, or it may emerge due to hematogenous dissemination of the pathogen from another source, particularly in the pediatric population. Especially in hematogenous osteomyelitis in which osteoblast-rich and highly vascularized growth plate is involved, complete treatment is quite challenging, and recurrence is very frequent [1].

The effects of the immune system on bone tissue have been an important subject of research since its discovery a few decades ago that IL-1β triggers bone destruction [3]. In addition to IL-1β, cytokines such as IL-17 and TNF-α also play a significant role in this process. Several bacterial agents involved in the etiology of osteomyelitis trigger an immune response by secreting toxins, leading to the release of these cytokines and contributing to bone destruction. The initial stage of osteomyelitis treatment entails prolonged antibiotic therapy along with surgical debridement. Since both osteomyelitis itself and its treatment can induce inflammatory responses and exacerbate bone loss [4], patients may benefit from immunomodulatory properties of alternative treatment options alongside conventional therapies, particularly in cases of lower treatment efficacy [5].

Dexmedetomidine (DXMT), a selective α2-adrenoreceptor agonist, has been demonstrated to elicit anxiolytic, hypnotic and sedative effects without the induction of respiratory depression. In addition to its anesthetic properties and its use in inducing semi-physiological sleep or sedation in critically ill patients in intensive care, neuroprotective, cardioprotective and renal protective effects have been demonstrated. Moreover, protective and healing effects, as well as antioxidant, anti-inflammatory and anti-apoptotic effects on various tissues and organs in different pathological processes, have been documented [6–13]. The administration of DXMT has been demonstrated to enhance the expression of genes associated with osteogenesis and angiogenesis while concurrently reducing the incidence of apoptosis in a multitude of experimental models [14–17].

The objective of this study was to demonstrate the effects of DXMT on the suppression of infection and enhancement of bone healing markers in an in vitro infection model created with osteoblast cells. Although the positive effects of DXMT on osteoblastic activity, bone regeneration and inflammation are well documented in the literature, evaluation of the applicable antimicrobial dose with the assessment of cytotoxic effects is absent. Therefore, varying doses of DXMT was administered to the SAOS-2 cell line infected with Gram-positive *S. aureus* to investigate the drug's impact on cytotoxicity to provide insights into the potential therapeutic benefits of DXMT in managing osteomyelitis.

Materials and methods

Culture and maintenance of osteosarcoma-derived osteoblast cells (SAOS-2)

In this study, osteoblast cells derived from the human osteosarcoma cell line (SAOS-2), procured from the Turkish ŞAP Institute, were utilized. All chemicals were purchased from Merck KGaA, (Darmstadt, Germany) unless otherwise stated. The cells were cultured in DMEM/Ham's F-12 medium supplemented with 10% Fetal Bovine Serum (FBS), 1% Penicillin–Streptomycin, and 1% Amphotericin-B. Cultures were maintained under standard conditions at 37 °C in a humidified atmosphere with 5% CO_2. Upon reaching 80% confluency, the cells were re-seeded, and the lag phase as well as the Population Doubling Time (PDT) were calculated and given as a Supplementary Figure (Supp. Figure 1). The experimental time intervals for infection control were subsequently determined based on the PDT (24,6 h) and its doubling which refer to 24 and 48 h, approximately.

Differentiation and characterization of SAOS-2 cells for *S. aureus* susceptibility

To enhance susceptibility to *S. aureus* infection, an osteocyte-like phenotype was induced following the protocol described by Gunn et al. [18]. Briefly, the culture medium was supplemented with 1.8 mM potassium dihydrogen phosphate, and the cells were transitioned into this differentiation medium. The cells were maintained under standard culture conditions (5% CO_2 and 37 °C) for a duration of 28 days to facilitate differentiation.

On the 28th day, the differentiated cells were characterized through quantitative PCR (qPCR) to assess alterations in the expression of biomarkers associated with early osteogenesis and osteocyte-like differentiation. The osteoblast-specific markers evaluated included RUNX2 (Runt-related transcription factor 2) and SP7 (Specifity Protein 7) [19–21]. In addition, markers indicative of osteocyte-like differentiation, such as RANKL (Receptor Activator of Nuclear Factor Kappa-B Ligand) and SOST (Sclerostin) were quantified with qPCR [22–24]. Primers are listed as a Supplementary Table (Supp. Table 1).

RNA isolation

The medium of SAOS-2 cells, whose RNA is to be isolated, was removed, and the cells were lysed using 1 mL

TRIzol Reagent. Following centrifugation at 12,000 g for 10 min at 4˚C, the aqueous phase containing RNA was transferred to a new tube. For phase separation, 100 µL BCP (1-bromo-3-chloropropane) was added, vortexed for 15 s, and incubated at room temperature for 10 min. The sample was then centrifuged again at 12,000 g for 10 min at 4˚C. RNA was present in the supernatant. To the transferred supernatant, 500 µL isopropanol was added, vortexed for 5–10 s, and incubated at room temperature for 15 min. At this stage, a white RNA pellet was expected to form. The RNA pellet was washed with 1 mL of 75% ethanol and centrifuged at 7,500 g for 5 min at room temperature to remove the alcohol. The RNA pellet was then dissolved in 100 µL nuclease-free water.

cDNA synthesis

cDNA was synthesized from 1 µg of total RNA using the Roche Transcriptor First Strand cDNA Synthesis Kit with random hexamers in a total reaction volume of 20 µL.

qPCR

qPCR was performed using LightCycler® 480 SYBR® Green I Master on the Roche LightCycler® 480 platform with three biological and three technical replicates. Relative gene expression was calculated using the 2-ΔΔCt method. Gene expression levels were normalized to the endogenous control, GAPDH.

Establishment of *S. aureus* infection in osteocyte-like differentiated SAOS-2 cells

S. aureus ATCC 43300 (MRSA) stock culture was activated in Tryptic Soy Broth (TSB) medium at a 1% inoculation rate and incubated at 37 °C for 24 h. Following the 24-h incubation, the cultures were inoculated into the cell line to achieve an OD600 value of 0.5. Prior to inoculation, the active culture was centrifuged at 10,000 g for 10 min to obtain the pellet, which was washed twice with Phosphate Buffered Saline (PBS). The washed pellet was resuspended in an equal volume of PBS and added to the cell line.

Bacterial enumeration was performed by preparing serial dilutions of the culture and spreading them onto Tryptic Soy Agar (TSA, Merck) plates. After 24 h of incubation at 37 °C, the bacterial count per milliliter was calculated.

The bacteria were incubated with host cells at 37 °C for 2 h, followed by two PBS washes. To eliminate extracellular bacteria, the cultures were treated with 10 µg/mL lysostaphin and incubated at 37 °C for 2 h. The experiment was carried out over a 7-day period, during which the culture medium was replaced daily.

To quantify intracellular bacteria, the infected cultures were lysed using 0.2% Triton X-100 in water at 37 °C for 20 min. Serial dilutions of the lysates were plated onto TSA plates and incubated at 37 °C for up to 120 h. Bacterial counts were recorded at the 24th and 120th hours of incubation to evaluate both rapid and slow growth rates [25]. After infection was confirmed, drug-treated and untreated media were introduced to the cells, and at the 24th and 48th hours, TSA plating was performed to investigate the presence of extracellular bacterial growth.

Optimization of dexmedetomidine administration and dosing protocols

The aim of this study was to evaluate the antimicrobial and anti-inflammatory effects of DXMT in an in vitro osteomyelitis model, with a simultaneous assessment of its cytotoxic effects through the measurement of reactive oxygen species (ROS) production and cell viability. The antimicrobial dose of DXMT for *S. aureus* had been previously reported in the literature as 32 µg/mL, though this study did not include host cells [23]. In subsequent research using osteoblast cells, lower DXMT concentrations ranging between 0.1 and 10 µM were employed [18, 25–27] To prioritize the assessment of antimicrobial efficacy, the highest dose, 10 µM, was selected as the initial test concentration. Additional concentrations of 0.1, 0.3, 1, 2, and 5 µM were also evaluated on control and infection positive groups to mitigate potential cytotoxic effects of higher doses on host cells.

Investigation of the therapeutic effects of DXMT

Assessment of cellular activity

The WST-1 assay, a colorimetric method to assess cell viability via the measurement of the metabolic activity of the cells was evaluated to address cytotoxicity. Following DXMT treatment, cells were trypsinized, centrifuged, and seeded into 96-well plates at an optimized density to ensure confluency did not exceed 80% during the assay. The WST-1 reagent was prepared according to the manufacturer's instructions and stored under appropriate conditions until use.

The reagent was added to each well at a volume corresponding to 10% of the total well volume. The plates were gently mixed to ensure even distribution of the reagent and incubated at 37 °C for 2 h. During this time, the WST-1 reagent was enzymatically reduced by mitochondrial enzymes in viable cells, forming a yellow-colored formazan product proportional to the number of metabolically active cells.

After the incubation period, the absorbance of the formazan product was measured at 450 nm using a microplate reader, with background readings subtracted to ensure accuracy. The data were normalized to untreated control groups, and cell viability was expressed as a percentage relative to these controls. Negative

controls (wells containing medium without cells) and positive controls (wells containing untreated viable cells) were included to validate the assay. Each experimental condition was performed in triplicate to ensure reproducibility.

Quantification of Reactive Oxygen Species (ROS) levels

ROS levels were visualized and quantified using a Carl-Zeiss LSM-510 confocal microscope equipped with 488 nm Argon, 543 nm He–Ne, and 633 nm He–Ne lasers and a 63×Zeiss Plan-Apo objective. Osteoblast cells were loaded with 10 µM cell-permeable 2',7'-dichlorodihydrofluorescein diacetate (H_2DCFDA) for 60 min at room temperature, following the protocol described by Tuncay and Turan [28]. After exposure to 100 µM H_2O_2, the maximum fluorescence intensity from 10 randomly selected fields, each containing 30–70 cells, was measured. These values were compared with basal fluorescence levels for each cell. The data obtained were then analyzed comparatively across the experimental groups.

Quantification of inflammatory cytokine levels

Inflammatory cytokines associated with osteomyelitis, either induced or inhibited, had been previously identified in the literature [3, 4]In this study, pro-inflammatory cytokines, including IL-1β, IL-6, IL-17, and TNF-α (were quantified using ELISA kits purchased from Elabscience, Houston, Texas.

Quantification of osteogenic markers of bone healing

Bone healing was determined with the quantification of osteogenic markers [BMPR1A (Bone Morphogenetic Protein Receptor Type 1), BMPR1B (Bone Morphogenetic Protein Receptor Type 1B), MMP2 (Matrix Metallopeptidase 2)] with ELISA kits purchased from MyBiosource, Inc. (San Diego, CA, USA) following DXMT treatment on infectious osteoblast cells.

ELISA assay

For the quantification of inflammatory cytokine levels and osteogenic markers cells designated for the experimental groups were seeded into 6-well culture plates prior to the establishment of infection conditions. Following exposure to drug-treated or untreated conditions, cells were centrifuged at 150 g for 10 min at the 24th and 48th hours. Pro-inflammatory cytokine levels in the supernatant were measured spectrophotometrically at 450 nm, with a separate ELISA assay performed for each cytokine in 96-well plate set ups.

The negative control group was exposed exclusively to poly-L-arginine hydrochloride for 48 h. All measurements were conducted at the highest concentration of each experimental group. The resulting data were analyzed comparatively among the groups.

Statistical analysis

Data were analyzed using GraphPad Prism (version 8.2.1). Statistical significance was assessed using two-way analysis of variance (ANOVA). Tukey's multiple comparisons test was performed to identify specific group differences. Results are presented as mean ± standard deviation (SD). A p-value of < 0.05 was considered statistically significant.

Results

Characterization of the osteocyte-like differentiation of the SAOS-2 cells

For the characterization of the SAOS-2 cells following differentiation to an osteocyte-like stage, osteoblast and osteocyte markers were quantified with qPCR before and after the application of the differentiation protocol. While osteoblast markers (RUNX2 and SP7) were down-regulated in osteocyte-like SAOS-2 cells compared to the undifferentiated stage ($p < 0.0001$), osteocyte markers (RANKL and SOST) were up-regulated significantly ($p < 0.0001$). These results indicate that we have successfully altered the phenotype of our target cells along with changes at the cellular level (Fig. 1).

Effects of DXMT on cellular activity

To understand whether applicable doses of DXMT are cytotoxic or not, osteocyte-like SAOS-2 cells were treated with 0.1–10 µM DXMT for 24 h. Although cellular activity was not affected by low doses up to 1 µM, viable cell number decreased with DXMT administration ≥ 5 µM. Viable cell numbers were as follows for osteocyte-like SAOS-2 cells for 1, 2, 5 and 10 µM DXMT doses: 0.32 ± 0.03, 0.29 ± 0.04, 0.21 ± 0.03 and $0.19 \pm 0.01 \times 10^4$. Cell number significantly decreased compared to the control group with increasing doses ($p = 0.0025$, $p = 0.0002$, $p < 0{,}0001$ and $p < 0{,}0001$ for 1, 2, 5 and 10 µM DXMT doses, respectively) (Fig. 2).

Antimicrobial properties of DXMT on osteocyte-like SAOS-2 cells

For the determination of optimum antimicrobial dose on osteocyte-like SAOS-2 cells infected with *S. aureus* DXMT doses ranging from 0.1–10 µM were tested. 0.1–2 µM doses and 10 µM dose showed no antimicrobial effects on any experimental groups. The counts (CFU/mL and l*og* values) of *S. aureus* ATCC 43300 in the medium following the application of 0, 5, and 10 µM doses of DXMT on osteocyte-like SAOS-2 cells at 37 °C after 24 and 48 h of incubation were summarized in Table 1.

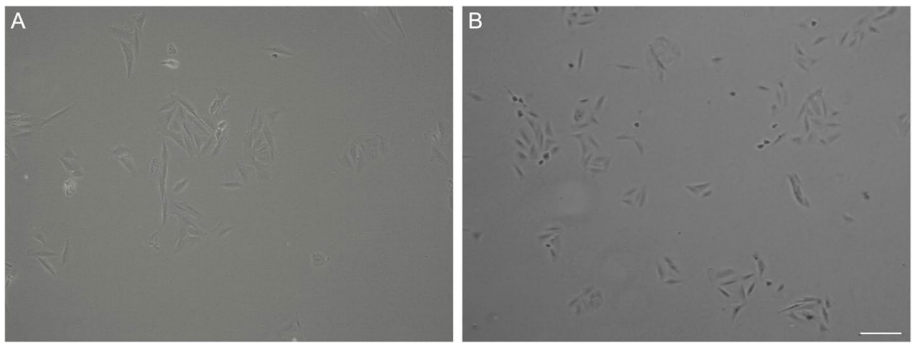

Fig. 1 **A** Osteoblast and **B** Osteocyte—like SAOS-2 cells following 28 days of incubation with 1.8 mM potassium dihydrogen phosphate visible with their typical phenotypes. Scale bar: 100 µm

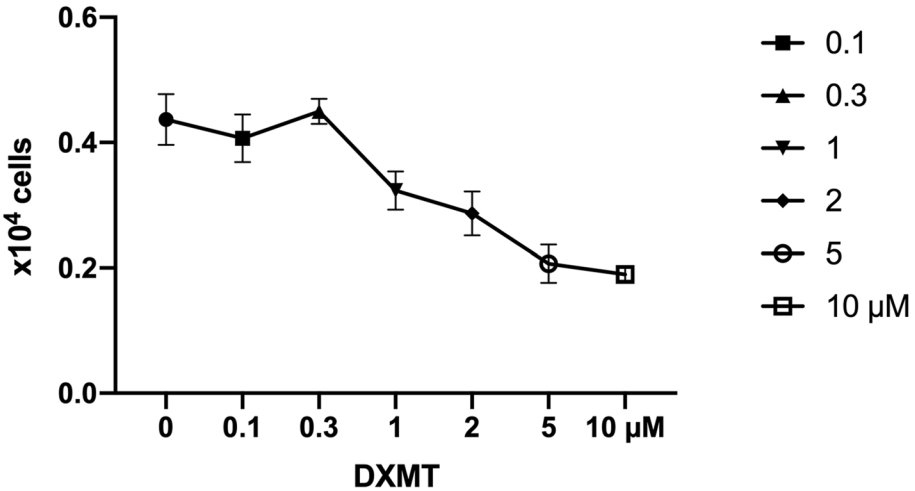

Fig. 2 WST-1 assay results at 450 nm absorbance for numbers of viable DXMT-treated osteocyte-like SAOS-2 cells

The enumeration results revealed that, particularly in the intracellular bacterial counts, there was a slight reduction in the bacterial load in the samples treated with 5 µM dose compared to the controls. For the 24-h incubation period, the intracellular bacterial count in the control sample was calculated as 6.2 *log*, while the count for the sample treated with 5 µM DXMT was determined as 6.1 *log*. After 48 h of incubation, the counts for these samples were calculated as 6.9 *log* and 6.3 *log* for control and 5 µM DXMT groups, respectively (Fig. 3).

Effects of DXMT on Reactive Oxygen Species (ROS) production

To evaluate the cytotoxic effects of DXMT on osteocyte-like SAOS-2 cells, DXMT doses ranging between 0.1–10 µM was tested on infection negative and positive groups.

In the *S. aureus* (-) group, ROS production increased by 1.35 ± 0.29-fold at 5 µM DXMT and 1.38 ± 0.42-fold at 10 µM DXMT, suggesting a cytotoxic effect of DXMT on osteoblast-like cells.

A significant increase in ROS levels was observed in the *S. aureus* (+) control group compared to *S. aureus (-)* control group ($p < 0{,}0001$). Administration of 5 µM DXMT revealed a significant reduction in ROS levels on cells infected with *S. aureus*. However, when *S. aureus* (+) cells were treated with 10 µM DXMT ROS levels were elevated rather than diminished. Furthermore, direct comparison between the *S. aureus* (+) control, 5 µM and 10 µM DXMT groups demonstrated that the lowest ROS levels were observed in the 5 µM group (Fig. 4).

Effects of DXMT on inflammatory pathways

Anti-inflammatory effects of varying DXMT doses on *S. aureus* infection was demonstrated with ELISA test for specific inflammatory cytokines. Within these cytokines, IL-1β and TNF-α levels significantly increased following *S. aureus* infection at 24 h ($p = 0.0007$ and $p = 0.0012$,

Table 1 CFU/mL and log values for *S. aureus* ATCC 43300 in DXMT treated osteocyte-like SAOS-2 cells

Infection status	Incubation time	Cell count	DXMT dose	Cell count (kob/mL)	Cell count (logarithmic)	Fold change (compared to the controls)
S. aureus (+)	24 h	Extracellular	0	1.9×10^{7}	7,3 *log*	-
			5	4.0×10^{7}	7,6 *log*	0,3 *log* increase
			10	4.7×10^{7}	7,7 *log*	0,4 *log* increase
		Intracellular	0	1.5×10^{6}	6,2 *log*	-
			5	1.3×10^{6}	6,1 *log*	0,1 *log* decrease[a]
			10	1.6×10^{6}	6,2 *log*	1
	48 h	Extracellular	0	1.6×10^{10}	10,2 *log*	-
			5	2.5×10^{10}	10,4 *log*	0,2 *log* increase
			10	1.6×10^{10}	10,2 *log*	1
		Intracellular	0	8.5×10^{6}	6,9 *log*	-
			5	2.2×10^{6}	6,3 *log*	0,6 *log* decrease*
			10	9.0×10^{6}	6,95 *log*	0,05 *log* increase
S. aureus (-)	24 h	Extracellular	0	< 10 kob/mL	< 1 *log*	-
			5	< 10 kob/mL	< 1 *log*	-
			10	< 10 kob/mL	< 1 *log*	-
		Intracellular	0	< 10 kob/mL	< 1 *log*	-
			5	< 10 kob/mL	< 1 *log*	-
			10	< 10 kob/mL	< 1 *log*	-

[a] Logarithmic decrease in cell count pointing to an antimicrobial effect compared to the controls was revealed at 5 µM dose at both time points

respectively) and 48 h ($p<0.0001$). 10 µM DXMT reduced IL-1β levels significantly (15.00 ± 1.00 vs. 5.00 ± 1.00 pg/mL for infected and non-infected groups, respectively, Fig. 5A), but not TNF-α (118.33 ± 6.66 vs. 95.00 ± 1.00 pg/mL, $p=0.0144$, Fig. 5B). At 48 h, IL-1β and TNF-α levels were similar between infectious and non-infectious groups following 5 and 10 µM DXMT administration indicating an anti-inflammatory effect (Fig. 5A and B).

Dose-dependent effects of DXMT varied between cytokines. A significant reduction in inflammation was observed starting from 0.3 µM for IL-6 ($p=0.0271$, Fig. 5D), 2 µM for IL-1β ($p=0.0247$, Fig. 5A) and IL-17 ($p=0.0118$, Fig. 5C), and 10 µM for TNF-α ($p=0.0137$, Fig. 5B) at 24 h. At 48 h, significant reductions occurred starting at 0.1 µM for IL-17 ($p=0.0022$) and IL-6 ($p=0.0022$, Fig. 5C and D) and at 0.3 µM for IL-1β ($p=0.0212$, Fig. 5A) and TNF-α ($p<0.0001$, Fig. 5B). Notably, IL-6 and IL-17 levels did not align with controls at any time point for 5 and 10 µM doses (Fig. 5C and D).

Effects of DXMT on bone healing and regeneration

Levels of osteogenic markers were compared between non-infectious osteocyte-like SAOS-2 cells and *S. aureus* (+) cells following DXMT administration for 5 and 10 µM doses where both antimicrobial and anti-inflammatory effects were determined. Levels of all three osteogenic markers that were tested was decreased with infection ($p<0.0001$, Fig. 6). In *S. aureus* (+) groups protein concentrations for BMPR1A and BMPR1B were significantly increased with 5 ($p=0.0184$ and $p=0.0343$, respectively) and 10 µM ($p=0.0010$ and $p=0.0041$, respectively) DXMT administration, while MMP2 levels (818.33 ± 155.2 pg/mL) were increased only with 10 µM dose compared to the *S. Aureus* (+) controls ($p=0.0183$).

Discussion

In this study, we investigated the antimicrobial and anti-inflammatory effects of DXMT using an in vitro bone infection model. Our results demonstrated that DXMT exerts dose-dependent effects on cell viability, ROS production, and inflammatory cytokine levels in *S. aureus* infected osteoblast-like cells. While DXMT at 5 µM reduced intracellular bacterial load and decreased ROS production, higher doses exhibited cytotoxic effects, indicating a fine balance between therapeutic benefits and potential cellular toxicity. These findings provide critical insights into DXMT's potential role in osteomyelitis treatment.

Aside from its sedative and hypnotic effects, clinical trials have demonstrated that DXMT suppresses inflammatory cytokines such as TNF-α and IL-6 in both in vitro and in vivo settings [29]. Our findings align with these studies, further highlighting DXMT's immunomodulatory properties, particularly in relation to IL-1β and IL-17

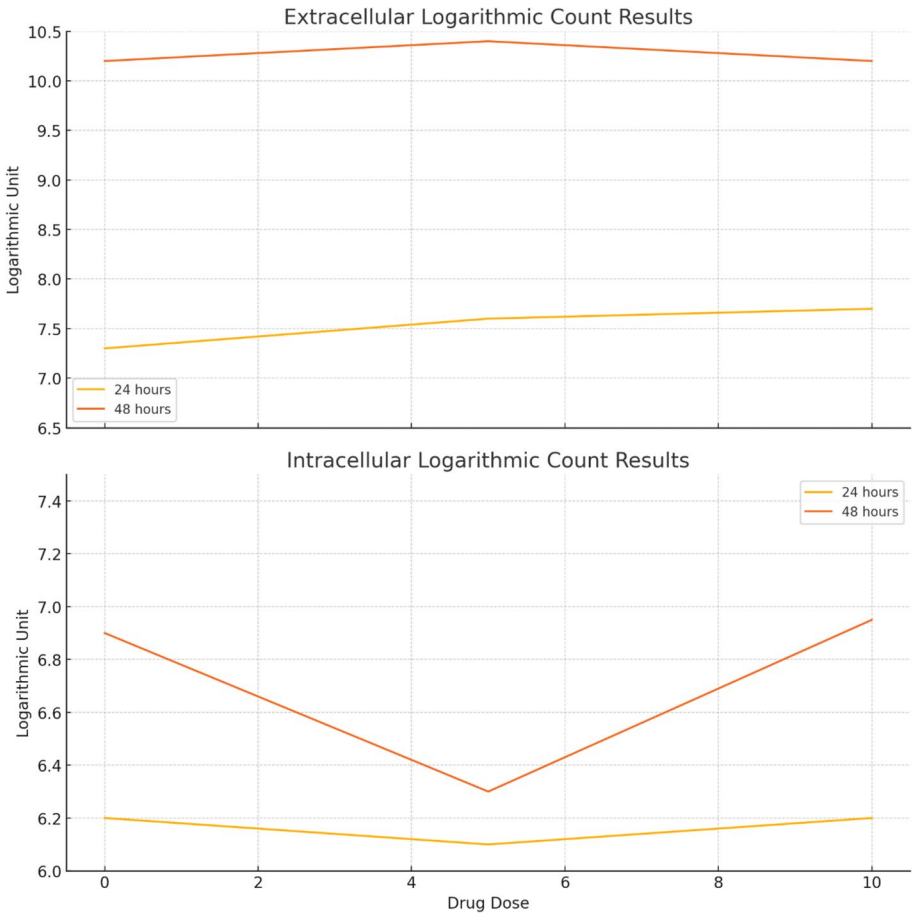

Fig. 3 The logarithmic changes in bacterial counts in the experiment conducted with osteocyte-like SAOS-2 cells infected and non-infected with *S. aureus* ATCC 43300 bacteria, were analyzed both extracellularly and intracellularly at 5 and 10 µM DXMT doses following 24 and 48 h of incubation. The logarithmic cell count revealed an optimum antimicrobial effect at 5 µM dose compared to the controls

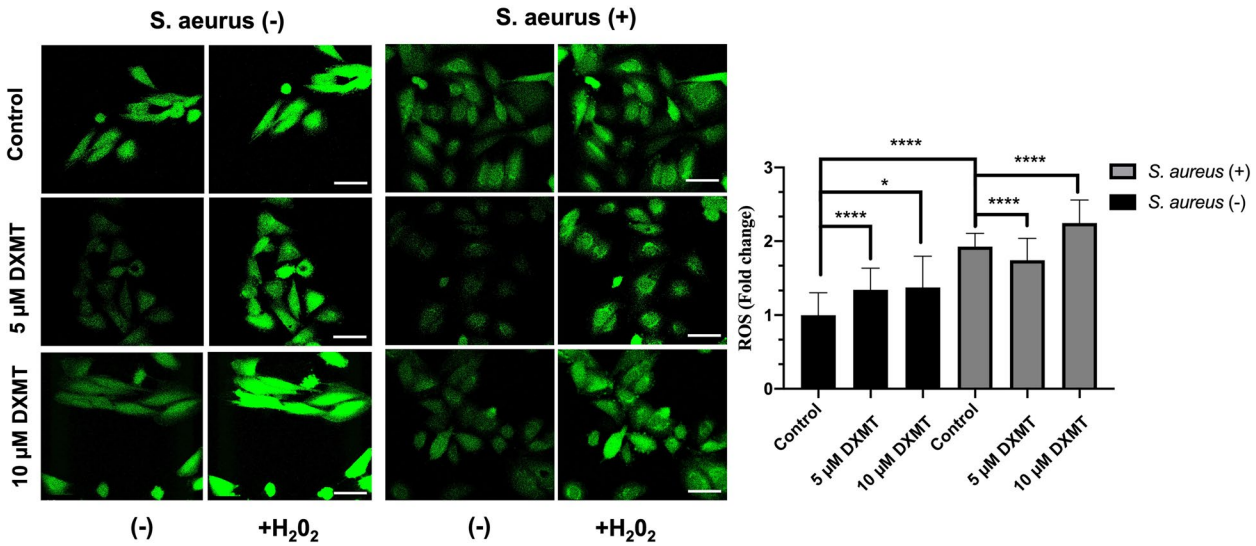

Fig. 4 Effects of DXMT administration on ROS production in *S. aureus* (-) and *S. aureus* (+) osteocyte-like SAOS-2 cells. Higher fluorescent intensity indicates a decrease in ROS levels. When fluorescent intensity was calculated it was demonstrated that DXMT at 5 and 10 µM doses were cytotoxic in non-infectious groups, while 5 µM DXMT administration was significantly effective on decreasing ROS production following *S. aureus* infection. $^{*}p < 0.05$, $^{****}p < 0.0001$. Scale bar: 10 µm

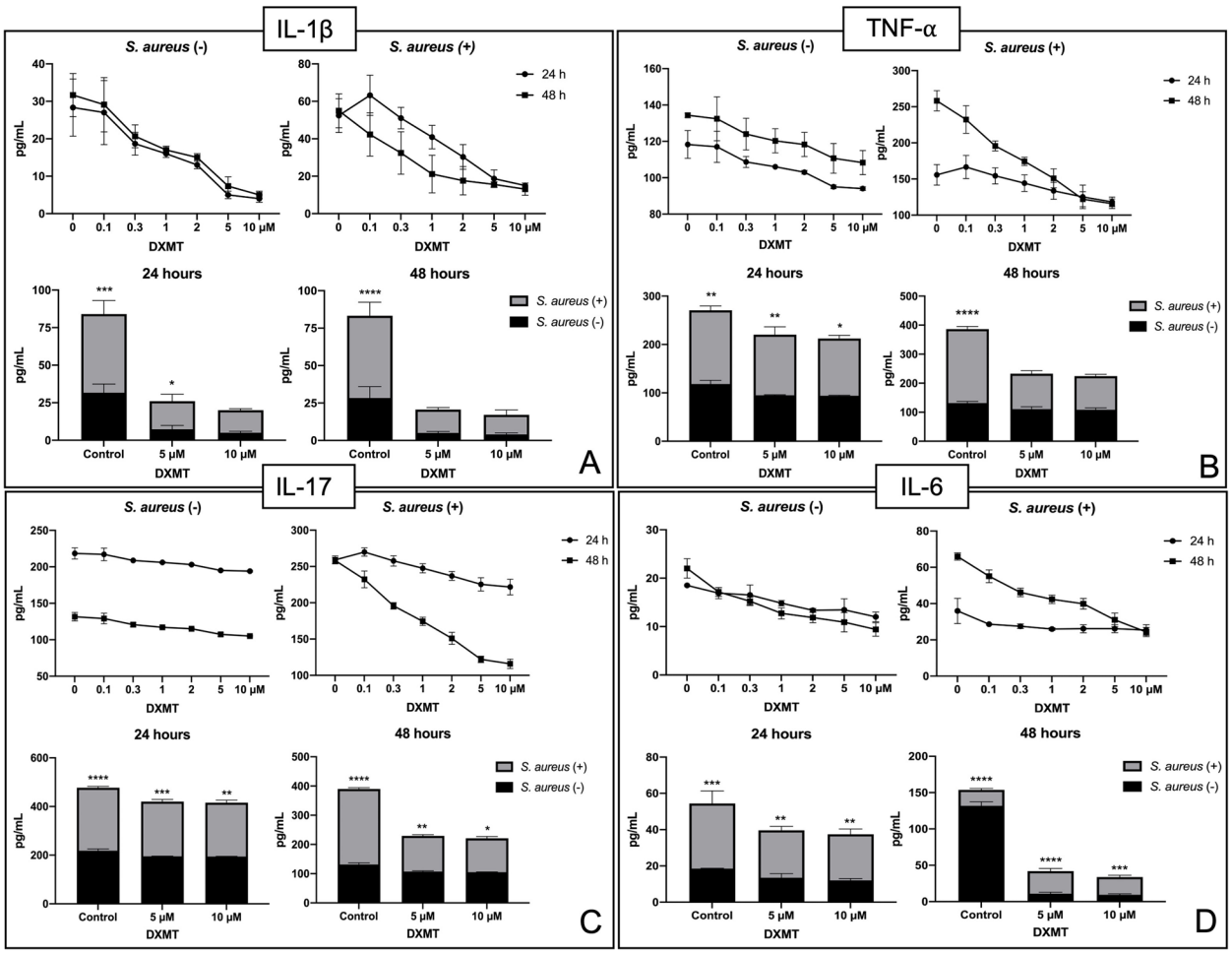

Fig. 5 Effects of 0.1–10 μM DXMT on inflammatory cytokines (**A**) IL-1β, (**B**) TNF-α, (**C**) IL-17, and (**D**) IL-6 measured via ELISA at 24 and 48 h in osteocyte-like SAOS-2 cells. *S. aureus* infection significantly increased cytokine levels at both time points, while DXMT reduced inflammation in a time-dependent manner at varying doses. *$p < 0.05$, **$p < 0.001$, ***$p < 0.005$, **$p < 0.0001$

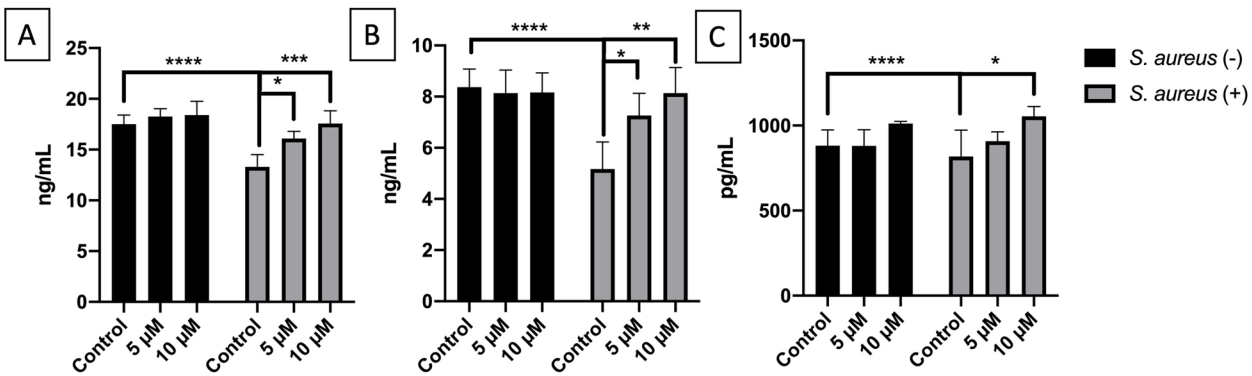

Fig. 6 Effects of 5 and 10 μM DXMT on osteogenic markers at 48 h on *S. aureus* (-) and *S. aureus* (+) osteocyte-like SAOS-2 cells determined with ELISA method for **A**) BMPR1A, **B**) BMPR1A, and **C**) MMP2 proteins

regulation. At doses of 0.1–5 μM, our results showed that the increase in inflammatory cytokine levels at 24 h was attributed to *S. aureus* infection, whereas the significant reduction observed at 48 h reflected DXMT's anti-inflammatory action compared to controls. This is consistent with previous research demonstrating that DXMT

significantly reduces inflammatory markers such as IL-1, IL-6, TNF-α, ESR, and CRP in patients with septic shock [8, 30]. However, at a 10 μM concentration, we observed that DXMT's cytotoxic effects impaired its immunomodulatory function, potentially disrupting the delicate balance between inflammation control and cell viability. These findings underscore the importance of adjusting in vivo doses based on in vitro cytotoxicity, as excessive concentrations may counteract the expected therapeutic effects over time.

Antibiotics such as cefazolin, clindamycin, and vancomycin have been successfully used in the treatment of various types of osteomyelitis in conjunction with surgery [31, 32]. Extending the treatment duration to six or even twelve weeks does not appear to make a significant difference [33]. In this case, prolonged antibiotic therapy could be recommended alongside antimicrobial agents to improve remission rates, which range between 60–90%, particularly benefiting patients with lower treatment efficacy [34]. The results of our study suggest that DXMT, due to its observed antimicrobial effect even in the early stages, may help reduce the treatment duration for *S. aureus* infections when used together with antibiotics as a part of the routine treatment. However, this needs to be validated through experimental studies, as one of the limitations of our study is the lack of evaluation of potential synergistic effects. The only in vivo study evaluated the effects of DXMT together with an antibiotic, lidocaine, further attenuated inflammatory responses and reduced postoperative pain in a study of patients undergoing laparoscopic hysterectomy [29]. On the contrary, in vivo studies demonstrating the antimicrobial effect of DXMT alone are limited to above, and in vitro studies can be misleading due to the absence of host cells in experiments using high doses of DXMT. For example, multiple studies investigating the antimicrobial effects of DXMT have reported varying doses ranging between 32–64 μg/mL [25, 35], which is significantly higher than the therapeutic dose demonstrated in our study, which is 5 μM in vitro. In this context, our study's identification of high-dose cytotoxicity provides valuable insights for optimizing DXMT's clinical application for osteomyelitis.

In our study, we evaluated the effects of 5 and 10 μM doses of DXMT on osteogenic markers, since *S. aureus* infection significantly reduced BMPR1, BMPR2, and MMP2 levels. DXMT administration increased BMPR1 and BMPR2 levels at both doses, whereas MMP2 levels were elevated only at the 10 μM dose. Nonetheless, these dose-independent findings are consistent with the existing literature, suggesting a potential mechanism that may promote bone healing in vivo. In a study examining morphine-induced oxidative damage in rat-derived osteoblasts, it was shown that DXMT could enhance bone healing by enhancing the Nrf2-mediated antioxidant system and the PI3K/Akt pathway [36]. Zhang et al. demonstrated the improvement of arthritic pain as a result of intraarticular DXMT administration in rats [37]. Subsequently, in a study by Cheng et al. repeated intraarticular administration of DXMT was shown to improve arthritic gait disturbance, pain scores and cartilage tissue damage in pathological examination with anti-inflammatory mechanisms papain-mediated osteoarthritis in rats [38]. As indicated by our study, further in vivo investigations are required to establish the non-cytotoxic dose range of DXMT and to optimize its osteogenetic potential through alternative strategies, with a particular emphasis on local applications.

In conclusion, these findings, along with our results, suggest that DXMT not only exhibits antimicrobial and immunomodulatory properties but may also contribute to bone healing through its effects on osteogenic markers and inflammatory regulation. However, further in vivo studies are necessary to elucidate its precise role in osteomyelitis treatment and to optimize its therapeutic application while minimizing potential cytotoxic effects.

Supplementary Information

The online version contains supplementary material available at https://doi.org/10.1186/s12891-025-08555-6.

Supplementary Material 1.

Supplementary Material 2.

Acknowledgements
N/A.

Authors' contributions
Study Design: M.H.K., D. A.T., G. C. D. Experimental Design: M.H.K., D. A.T., G. C. D. Experimental Procedures: D. A.T., G. C. D., E.T. and E.G.A. Data Collection: M.H.K., D. A.T., G. C. D. Statistical analysis: D. A.T., E.T. Writing the manuscript: M.H.K., D. A.T., G. C. D. Figure preparation: M.H.K., D. A.T., G. C. D. and E.T. All authors reviewed the manuscript.

Funding
This research did not receive any specific grants from funding agencies in the public or commercial sector.

Data availability
The datasets used and/or analyzed in this study are available from the corresponding author on reasonable request.

Declarations

Ethics approval and consent to participate
N/A.

Consent for publication
N/A.

Competing interests
The authors declare no competing interests.

Author details
[1]Department of Pediatric Dentistry, Faculty of Dentistry, Ankara University, Ankara 06560, Türkiye. [2]Ankara University, Stem Cell Institute, Ankara 06520, Türkiye. [3]Department of Basic Medical Sciences, Faculty of Dentistry, Ankara University, Incitas Street, Ankara 06560, Türkiye. [4]Ankara University, Biotechnology Institute, Ankara 06135, Türkiye. [5]Department of Biophysics, Faculty of Medicine, Ankara University, Ankara 06100, Türkiye. [6]Department of Interdisciplinary Neuroscience, Ankara University, Ankara 06100, Turkey.

Received: 17 January 2025 Accepted: 19 March 2025
Published online: 02 April 2025

References

1. Lew DP, Waldvogel FA. Osteomyelitis. Lancet. 2004;364(9431):369–79.
2. Tang RH, Yang J, Fei J. New perspectives on traumatic bone infections. Chin J Traumatol. 2020;23(6):314–8.
3. Horton JE, Raisz LG, Simmons HA, Oppenheim JJ, Mergenhagen SE. Bone resorbing activity in supernatant fluid from cultured human peripheral blood leukocytes. Science (1979). 1972;177(4051):793–5.
4. Pedersen JG, Lund B. Effects of gentamicin and monomer on bone. J Arthroplasty. 1988;3:S63–8.
5. Stallmann HP, Faber C, NieuwAmerongen AV, Wuisman PI. Antimicrobial peptides: review of their application in musculoskeletal infections. Injury. 2006;37(2):S34-40.
6. Bao N, Tang B. Organ-Protective Effects and the Underlying Mechanism of Dexmedetomidine. Mediators Inflamm. 2020;9(2020):1–11.
7. Yoon JY, Park JH, Kim EJ, Park BS, Yoon JU, Shin SW, et al. Dexmedetomidine attenuates H_2O_2-induced cell death in human osteoblasts. J Dent Anesth Pain Med. 2016;16(4):295.
8. Qiao H, Sanders RD, Ma D, Wu X, Maze M. Sedation improves early outcome in severely septic Sprague Dawley rats. Crit Care. 2009;13(4):R136.
9. Yeh YC, Wu CY, Cheng YJ, Liu CM, Hsiao JK, Chan WS, et al. Effects of dexmedetomidine on intestinal microcirculation and intestinal epithelial barrier in endotoxemic rats. Anesthesiology. 2016;125(2):355–67.
10. Peng K, Chen W, Xia F, Liu H, Meng X, Zhang J, et al. Dexmedetomidine post-treatment attenuates cardiac ischaemia/reperfusion injury by inhibiting apoptosis through HIF-1α signalling. J Cell Mol Med. 2020;24(1):850–61.
11. Cheng J, Zhu P, Qin H, Li X, Yu H, Yu H, et al. Dexmedetomidine attenuates cerebral ischemia/reperfusion injury in neonatal rats by inhibiting TLR4 signaling. J Int Med Res. 2018;46(7):2925–32.
12. Liang S, Wang Y, Liu Y. Dexmedetomidine alleviates lung ischemia-reperfusion injury in rats by activating PI3K/Akt pathway. Eur Rev Med Pharmacol Sci. 2019;23(1):370–7.
13. Bayram A, Erkan GN, Talih G, Baskol G, Deniz K, Yildiz K, et al. The alpha-2 receptor agonist dexmedetomidine attenuates vancomycin-induced acute kidney injury. Bratisl Lek Listy. 2019;120(6):429–33.
14. Wang Z, Ge X, Wang Y, Liang Y, Shi H, Zhao T. Mechanism of dexmedetomidine regulating osteogenesis-angiogenesis coupling through the miR-361-5p/VEGFA axis in postmenopausal osteoporosis. Life Sci. 2021;275:119273.
15. Fang B, Li XQ, Bi B, Tan WF, Liu G, Zhang Y, et al. Dexmedetomidine attenuates blood-spinal cord barrier disruption induced by spinal cord ischemia reperfusion injury in rats. Cell Physiol Biochem. 2015;36(1):373–83.
16. Fang M, He J, Ma X, Li W, Lin D. Protective effects of dexmedetomidine on the survival of random flaps. Biomed Pharmacother. 2020;1:128.
17. Suzuki S, Nishiwaki K, Nan YS, Li SY, Kang JL, Ema Y. Effects of midazolam, diazepam, propofol and dexmedetomidine on endothelial cell proliferation and angiogenesis induced by VEGF. Afr J Microbiol Res. 2010;4(23):2549–55. Available from: https://www.researchgate.net/publication/266276714.
18. Gunn NJ, Zelmer AR, Kidd SP, Solomon LB, Roscioli E, Yang D, et al. A human osteocyte cell line model for studying staphylococcus aureus persistence in osteomyelitis. Front Cell Infect Microbiol. 2021;3:11.
19. Komori T. Regulation of osteoblast differentiation by Runx2. Adv Exp Med Biol. 2010;658:43–9.
20. Agata H, Asahina I, Yamazaki Y, Uchida M, Shinohara Y, Honda MJ, et al. Effective bone engineering with periosteum-derived cells. J Dent Res. 2007;86(1):79–83.
21. Lee TJ, Jang J, Kang S, Jin M, Shin H, Kim DW, et al. Enhancement of osteogenic and chondrogenic differentiation of human embryonic stem cells by mesodermal lineage induction with BMP-4 and FGF2 treatment. Biochem Biophys Res Commun. 2013;430(2):793–7.
22. Heino TJ, Kurata K, Higaki H, Väänänen HK. Evidence for the role of osteocytes in the initiation of targeted remodeling. Technol Health Care. 2009;17(1):49–56.
23. Kulkarni RN, Bakker AD, Everts V, Klein-Nulend J. Inhibition of osteoclastogenesis by mechanically loaded osteocytes: involvement of MEPE. Calcif Tissue Int. 2010;87(5):461–8.
24. Noda S, Kawashima N, Yamamoto M, Hashimoto K, Nara K, Sekiya I, et al. Effect of cell culture density on dental pulp-derived mesenchymal stem cells with reference to osteogenic differentiation. Sci Rep. 2019;9(1):5430.
25. Ayoglu H, Kulah C, Turan I. Antimicrobial effects of two anaesthetic agents: dexmedetomidine and midazolam. Anaesth Intensive Care. 2008;36(5):681–4.
26. Maisat W, Han X, Koutsogiannaki S, Soriano SG, Yuki K. Differential effects of dexmedetomidine on Gram-positive and Gram-negative bacterial killing and phagocytosis. Int Immunopharmacol. 2023;120:110327.
27. Cui J, Zhao H, Wang C, Sun JJ, Lu K, Ma D. Dexmedetomidine attenuates oxidative stress induced lung alveolar epithelial cell apoptosis in vitro. Oxid Med Cell Longev. 2015;2015:358396.
28. Tuncay E, Turan B. Intracellular Zn(2+) increase in cardiomyocytes induces both electrical and mechanical dysfunction in heart via endogenous generation of reactive nitrogen species. Biol Trace Elem Res. 2016;169(2):294–302.
29. Xu S, Hu S, Ju X, Li Y, Li Q, Wang S. Effects of intravenous lidocaine, dexmedetomidine, and their combination on IL-1, IL-6 and TNF-α in patients undergoing laparoscopic hysterectomy: a prospective, randomized controlled trial. BMC Anesthesiol. 2021;21(1):3.
30. Mokhlesian M, Heydari F, Boskabadi SJ, Baradari AG, Ajami A, Alizadeh-Navaei R. The effect of dexmedetomidine on inflammatory factors and clinical outcomes in patients with septic shock: a randomized clinical trial. Clin Ther. 2025;47(1):e9-17.
31. Woods CR, Bradley JS, Chatterjee A, Copley LA, Robinson J, Kronman MP, et al. Clinical Practice Guideline by the Pediatric Infectious Diseases Society and the Infectious Diseases Society of America: 2021 Guideline on Diagnosis and Management of Acute Hematogenous Osteomyelitis in Pediatrics. J Pediatric Infect Dis Soc. 2021;10:801–44 Oxford University Press.
32. Kavanagh N, Ryan EJ, Widaa A, Sexton G, Fennell J, O'Rourke S, et al. Staphylococcal osteomyelitis: disease progression, treatment challenges, and future directions. Clin Microbiol Rev. 2018;31(2):e00084.
33. Besal R, Adamič P, Beović B, Papst L. Systemic antimicrobial treatment of chronic osteomyelitis in adults: a narrative review. Antibiotics. 2023;12:944 MDPI.
34. Rod-Fleury T, Dunkel N, Assal M, Rohner P, Tahintzi P, Bernard L, et al. Duration of post-surgical antibiotic therapy for adult chronic osteomyelitis: a single-centre experience. Int Orthop. 2011;35(11):1725–31.
35. Kocaturk O, DonmezOzkan H, PoyrazogluCoban E, Biyik H. Antimicrobial effects of dexmedetomidine and midazolam in bicarbonate buffer: an in vitro study. Cerrahpasa Medical Journal. 2020;43(3):69–74.
36. Lou Y, Zou L, Shen Z, Zheng J, Lin Y, Zhang Z, et al. Protective effect of dexmedetomidine against delayed bone healing caused by morphine via PI3K/Akt mediated Nrf2 antioxidant defense system. Front Pharmacol. 2024;15:15.
37. Zhang WS, Xu H, Xu B, Sun S, Deng XM, Zhang YQ. Antihyperalgesic effect of systemic dexmedetomidine and gabapentin in a rat model of monoarthritis. Brain Res. 2009;6(1264):57–66.
38. Cheng F, Yan FF, Liu YP, Cong Y, Sun KF, He XM. Dexmedetomidine inhibits the NF-κB pathway and NLRP3 inflammasome to attenuate papain-induced osteoarthritis in rats. Pharm Biol. 2019;57(1):649–59.

Publisher's Note